Directional vortex-flux bifurcation in polycrystalline $YBa_2Cu_3O_7$ rotated in a magnetic field

Liwen Liu and J. S. Kouvel
Department of Physics, University of Illinois at Chicago, Chicago, Illinois 60680

T. O. Brun
P-LANSCE, Los Alamos National Laboratory, Los Alamos, New Mexico 87545
(Received 31 August 1990)

Magnetization-vector measurements on a field-cooled polycrystalline sample of $YBa_2Cu_3O_7$ rotated in a magnetic field **H** at 4.2 K reveal an extraordinary behavior of $\mathbf{M}_P$, the penetrating (vortex-flux) component of the magnetization. Near $H=0.8$ kOe, as θ the sample-rotation angle relative to **H** is raised from zero to 360°, the magnitude of $\mathbf{M}_P$ descends to a small minimum at $\theta\approx 205°$, and then again at $\theta\approx 155°$, as θ is lowered back to 0°. At each minimum, the direction of $\mathbf{M}_P$ changes very rapidly. For H at a critical value, the minimum $\mathbf{M}_P$ reaches zero and its direction changes abruptly by 180°. This behavior signifies a separation of the vortex lines into two groups, one of which rotates rigidly with the sample, while the other maintains a range of orientations extending from that of **H** and thus rotates frictionally relative to the sample. The proportion of vortex lines in each group varies systematically with H. This directional vortex-flux bifurcation can readily arise from a broad distribution in the strength of the vortex-pinning forces. Simple model calculations based on this premise give excellent qualitative agreement with experiment.

INTRODUCTION

The discovery of high-T_c superconductors and their enormous technological potential have regenerated great interest in type-II superconductors in general. Questions about the detailed nature of the mixed (vortex) state have captured particular attention. While the phenomenon of viscous vortex-line motion (known as flux creep) has continued to be explored extensively,[1-6] other work has reached back to study, more carefully, the vortex states achieved under different experimental conditions. Most tellingly, the latter work has included measurements of magnetization[7] and torque[8,9] on superconducting samples rotated in fixed magnetic fields (**H**). Our particular contributions, which we believe are especially probing, have been to measure the magnetization components parallel and perpendicular to **H** simultaneously, thus determining the magnetization of the rotating sample as a vector. Some earlier experiments on rotating superconductors, though equivalent in principle, have been less direct.[10] Since our previous findings form an essential context for the new results to be reported in this paper, we will now describe some of their salient features.

By rotational magnetization-vector (**M**) measurements on polycrystalline samples of niobium[11] and $YBa_2Cu_3O_7$,[12] we showed that the measured **M** can be decomposed unambiguously into a penetrating vortex-flux component ($\mathbf{M}_P$) and a diamagnetic shielding component ($\mathbf{M}_D$).[13] Moreover, for both materials, $\mathbf{M}_D$ was found to be closely equal to $\chi_0\mathbf{H}$, where χ_0 is the initial diamagnetic susceptibility even when the external field **H** is much larger in size than the lower critical field H_{c1}. This equality was seen to be independent of whether the sample is initially zero-field cooled (ZFC), field cooled (FC), or in some hysteretic state. What does depend on the thermomagnetic history is the initial magnitude of $\mathbf{M}_P$ which, for the same H, is consistently larger in the FC case than in the ZFC case.

Upon subsequent rotation of the $YBa_2Cu_3O_7$ sample in a fixed **H**, we observed[12] that the torque exerted by **H** causes $\mathbf{M}_P$, the vortex magnetization, to gradually depart from rigid rotation with the sample, the departure being most pronounced in the ZFC case. This behavior showed that the vortex-pinning forces in the sample have a broad distribution in strength and that the average pinning force is weaker in the ZFC case. As the sample was rotated further, $\mathbf{M}_P$ was found to assume a fixed orientation relative to **H** and a constant magnitude, which are the same for both FC and ZFC states at the same H (5 kOe). Thus, the memory of the initial state vanishes as the vortex lines hop progressively (and dissipatively) to neighboring sets of pinning centers, thereby retaining a steady-state balance between the torques exerted by **H** and by the pinning centers in the rotating sample. Macroscopically, this vortex-hopping process is frictional and distinct from the viscous flux-creep process. Indeed, the latter process was negligible in these experiments and in those described below, which were all carried out at 4.2 K.

We are now using similar magnetization-vector measurements to explore the rotational behavior of the vortex flux in polycrystalline $YBa_2Cu_3O_7$ under a greater variety of conditions. As reported in this paper, we have encountered an extraordinary effect when the sample is rotated in certain fields applied during the initial cooling to 4.2 K. This effect is seen to manifest a separation of the vortex flux into two components of different average orientations and of relative magnitudes that change systemati-

cally with the field. Indeed, at a critical value of the field, the two components become equal in magnitude and, therefore, when one of them is turned to lie antiparallel to the other, the total vortex magnetization goes to zero. According to our simple model interpretation, this rather dramatic effect can be derived directly from a distribution in the strength of the pinning forces on the vortex lines.

EXPERIMENTAL RESULTS

For the polycrystalline sample of this study (the same sample we investigated earlier[12]) a small sintered piece of superconducting $YBa_2Cu_3O_7$ prepared at the Argonne National Laboratory was broken into a powder, combined with a thin adhesive, and die-pressed into a uniform disk (5-mm diam, 0.5 mm thick). The sample disk was mounted in our vibrating-sample magnetometer (VSM) such that it can be rotated by 360° about its axis (the vertical axis of vibration) normal to a fixed external field (**H**). For this geometry, the demagnetization effects are very small. Two sets of VSM pickup coils are positioned in quadrature, allowing us to simultaneously measure the components of the magnetization (**M**) parallel and perpendicular to **H** in the sample-disk plane.

Thus, as shown in Fig. 1 (inset), the sample magnetization is measured as a vector of magnitude M and orientational angle ϕ relative to **H**, as the sample rotation angle

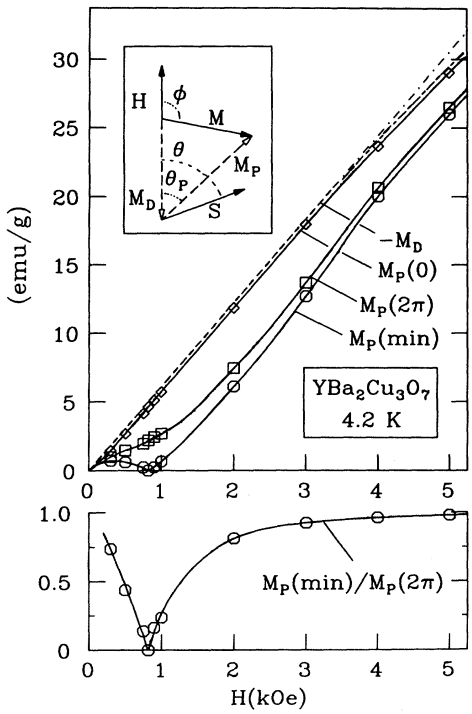

FIG. 1. $YBa_2Cu_3O_7$ cooled and measured in field H at 4.2 K. Inset: total magnetization **M** and its vortex-flux ($\mathbf{M}_P$) and diamagnetic ($\mathbf{M}_D$) components for sample S rotated by angle θ relative to **H**. M_P at $\theta=0$ and 2π, its minimum value, and $-M_D$ vs H. Below: $M_P(\text{min})/M_P(2\pi)$ vs H.

θ is typically cycled from 0° to 360° and back to 0°. As was done earlier[11,12] and is shown in the vector diagram, **M** is assumed to consist of two physically distinct components: a diamagnetic shielding component ($\mathbf{M}_D$) that stays antiparallel to **H** with fixed magnitude at constant H, and a penetrating vortex-flux component ($\mathbf{M}_P$). It is further assumed that $\mathbf{M}_P$ turns rigidly with the sample initially (i.e., that its orientational angle θ_P equals θ in the limit of very small θ) which follows if all the vortex lines are held by pinning forces, however weak some of the forces may be. This combination of physically reasonable assumptions allows us to establish the magnitude of $\mathbf{M}_D$ from our low-θ data and then to determine the variations in the size and direction of $\mathbf{M}_P$ over the entire sample-rotation cycle.

Following this procedure earlier[12] with our polycrystalline $YBa_2Cu_3O_7$ sample at 4.2 K and $H=5$ kOe, we found that M_D differs only slightly from $\chi_0 H$, as described above.[14] Moreover, in the FC case (i.e., when 5 kOe was also the field applied during cooling), we found that $M_P(0)$, the initial ($\theta=0°$) value of M_P, is nearly equal to $-M_D$. Hence, the Meissner effect, corresponding to $\mathbf{M}_P(0)+\mathbf{M}_D$, the sum of two large magnetization vectors in opposition, is nearly zero. When the field-cooled sample was then rotated, M_P was seen to drop to a lower value, where it remained for the rest of the rotational cycle.

These earlier results for $H=5$ kOe are shown in Fig. 1 in the context of our new findings for the $YBa_2Cu_3O_7$ sample cooled to 4.2 K in (and then rotated in) various lower values of H. We see that $-M_D$ varies linearly with H up to ~4 kOe, where the slope starts to decrease slowly from the value $-\chi_0$, and that $M_P(0)$ lies consistently just below $-M_D$, resulting in a Meissner effect that is very small and nearly constant over this range of H. Moreover, $M_P(2\pi)$, the M_P value at $\theta=360°$, is always considerably smaller than $M_P(0)$. However, for $H<5$ kOe, $M_P(2\pi)$ no longer represents a constant plateau value reached by M_P after its initial descent at low θ. Instead, M_P was seen to pass through a minimum value $M_P(\text{min})$ as θ was raised to 360° and then through a similar minimum as θ was returned to 0°. In fact, as shown in Fig. 1, $M_P(\text{min})$ goes essentially to 0 at H near 0.8 kOe. This interesting effect is brought out more vividly in the plot versus H of the ratio $M_P(\text{min})/M_P(2\pi)$.

In Figs. 2–4, the magnitude of the vortex-flux magnetization $\mathbf{M}_P$ and its orientational angle θ_P are displayed as functions of the sample-rotation angle θ for different values of H, the field applied during cooling and maintained during the sample rotations at 4.2 K. Well below the lowest H represented (0.5 kOe), M_P decreases at low θ and then remains at a constant value, while θ_P follows θ very closely, showing that the vortex flux rotates rigidly with the sample. Well above the highest field (1.0 kOe) and as reported earlier[12] for $H=5$ kOe, M_P undergoes the same simple change but θ_P rises to a small plateau value as θ increases to 360° and then descends to a negative plateau of the same size as θ decreases to 0°, thus exhibiting a frictional rotation of $\mathbf{M}_P$ relative to the sample. At intermediate values of H, as the figures clearly testify, the

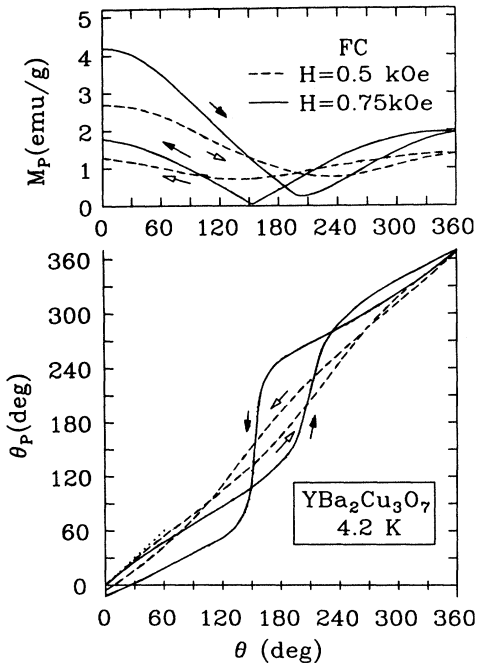

FIG. 2. Vortex-flux magnetization magnitude M_P and orientational angle θ_P vs rotational angle θ of $YBa_2Cu_3O_7$ sample cooled and measured in $H=0.5$ kOe (dashed curves) and 0.75 kOe (solid curves) at 4.2 K.

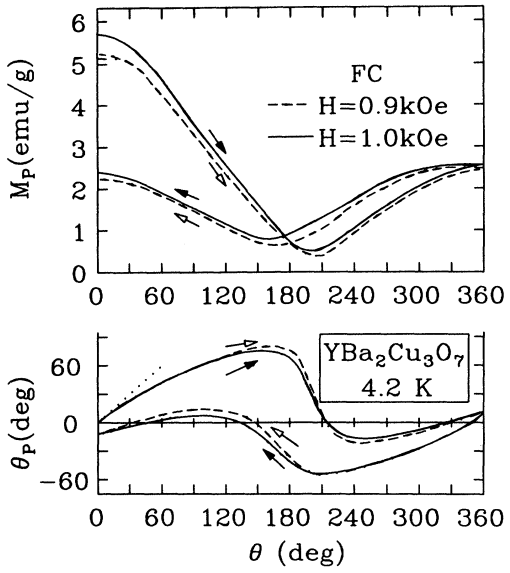

FIG. 4. Same as Fig. 2, except that $H=0.9$ kOe (dashed curves) and 1.0 kOe (solid curves).

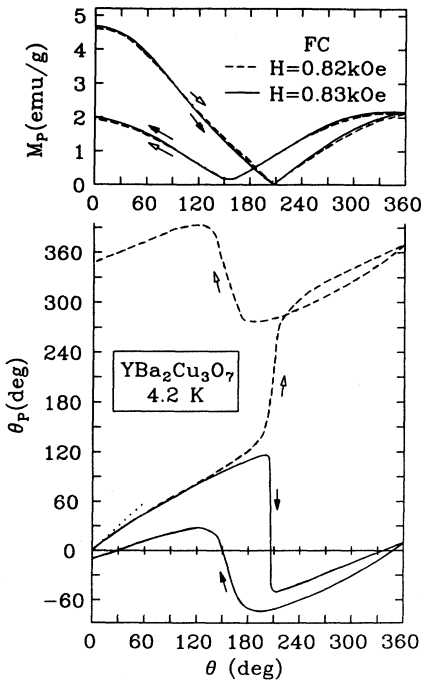

FIG. 3. Same as Fig. 2, except that $H=0.82$ kOe (dashed curves) and 0.83 kOe (solid curves).

rotational changes of the vortex-flux magnetization experience a remarkable evolution.

Starting with Fig. 2, we see that, as H is raised from 0.5 to 0.75 kOe, the small hysteresis in θ_P versus θ grows into large rapid changes near 180°±25° and that the minima in M_P, which occur at the same two θ values, become much deeper. Figure 3 shows that, for $H=0.82$ kOe, this process has progressed, except that, for the reverse rotation, the rapid change of θ_P has reversed in direction, and that, for $H=0.83$ kOe, the rapid θ_P changes have reversed in direction for both the forward and reverse rotations. For both these fields, the minima in M_P are very deep, reaching, in fact, to 0 for the forward rotation at 0.83 kOe, where the θ_P change at the same θ is virtually discontinuous and close to 180° in magnitude. Finally, in Fig. 4, we see that, when H is raised further to 0.9 and 1.0 kOe, the θ_P changes become more gradual and the M_P minima less pronounced, thus heading at higher H towards the simple frictional behavior of $\mathbf{M}_P$ described earlier for $H=5$ kOe.

It should be noted that these anomalies in the rotational properties of $\mathbf{M}_P$ are observed specifically for the field-cooled state of the $YBa_2Cu_3O_7$ sample within a certain range of fields. At all fields, including those within this range, the rotational behavior of $\mathbf{M}_P$ for the zero-field-cooled state at 4.2 K follows the simple frictional pattern seen for the FC state at high fields. Our ZFC results are exemplified by those for $H=0.7$ kOe shown in Fig. 5, where the variations of M_P and θ_P with θ are qualitatively very similar to what was observed for the FC state at 5 kOe, aside from the fact that M_P increases rather than decreases at low θ. That the ZFC behavior may exhibit some of the pecularities of the FC behavior, but at much lower fields, is not possible because $H_{c1}\approx 0.4$ kOe, below

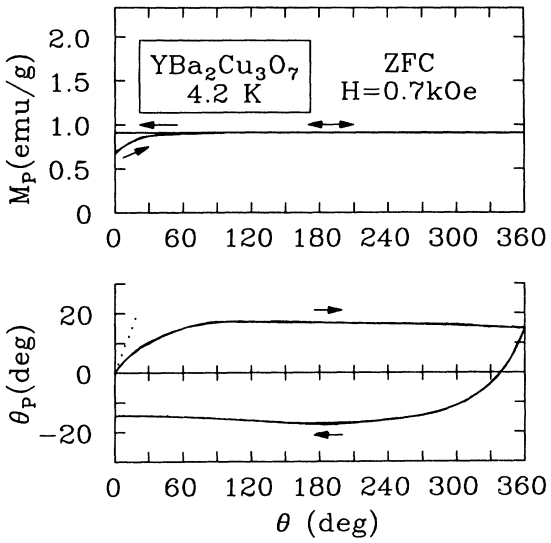

FIG. 5. Vortex-flux magnetization magnitude M_P and orientational angle θ_P vs rotational angle θ of $YBa_2Cu_3O_7$ sample measured in $H=0.7$ kOe at 4.2 K after zero-field cooling.

which $M_P=0$ in the ZFC state.

For the FC state, the peculiar features of the rotational behavior of $\mathbf{M}_P$ change very systematically with H, as can be readily seen in Fig. 6. Here, the $M_P(\min)/M_P(2\pi)$ ratio and $(d\theta_P/d\theta)^{-1}_{\max}$, the inverse of the maximum θ_P versus θ slope, are plotted against H for both the forward (F) and reverse (R) sample rotations. (For these plots, data taken at 0.80 and 0.84 kOe have also been used.) It is very evident that, for each direction of sample rotation, $M_P(\min)/M_P(2\pi)$ descends to 0 at the same critical value of H at which $d\theta_P/d\theta^{-1}_{\max}$ passes through 0 as it changes sign. For the F and R rotations, the critical values of H are 0.83 and 0.79 kOe, respectively, and the curves remain displaced along the H axis. Note that the $M_P(\min)/M_P(2\pi)$ versus H curve for the F rotation is an expansion about the critical H of the curve shown at the bottom of Fig. 1.

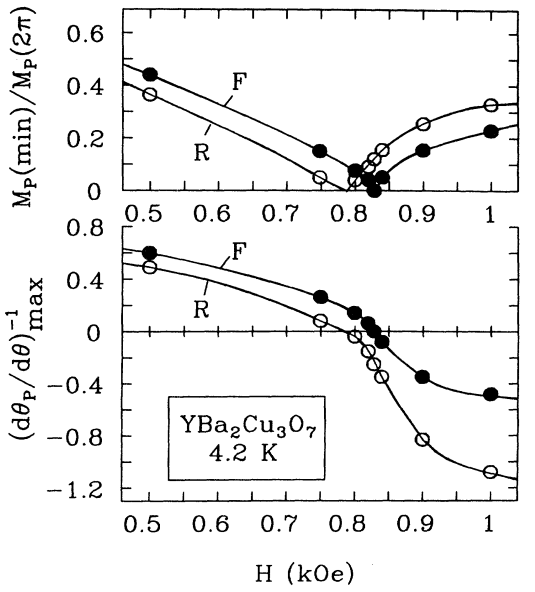

FIG. 6. $M_P(\min)/M_P(2\pi)$ and $(d\theta_P/d\theta)^{-1}_{\max}$ vs H for forward (F) and reverse (R) rotations of $YBa_2Cu_3O_7$ sample cooled in field H to 4.2 K.

The correlated variations of $M_P(\min)/M_P(2\pi)$ and $(d\theta_P/d\theta)^{-1}_{\max}$ with H, plus the fact that, when $(d\theta_P/d\theta)^{-1}_{\max}=0$, the abrupt θ_P change is 180°, strongly suggest that the observed $\mathbf{M}_P$ consists of two vectors, whose magnitudes are equal at the critical H and which become antiparallel as the sample is rotated. It was further recognized that these two vectors represent a bifurcation in the average orientation of the vortex flux, which can arise from a distribution in the strength of the vortex-pinning forces. In the following section, model calculations based on this simple premise are shown to reproduce all the salient features of the rotational properties just described for the vortex-flux magnetization of field-cooled polycrystalline $YBa_2Cu_3O_7$.

COMPARISON WITH MODEL CALCULATIONS

Consider a superconducting sample containing pinning centers that can exert a maximum torque τ_v on a vortex line of moment μ_v and that the sample is rotated by angle θ relative to $\mathbf{H}$, the external field. If $\tau_v \geq \mu_v H \sin\theta$ (the torque exerted by $\mathbf{H}$), the vortex line will turn rigidly with the sample, so that θ_v (its angle with $\mathbf{H}$) will stay equal to θ, whereas if $\tau_v < \mu_v H \sin\theta$, the vortex line will turn frictionally in the sample towards $\mathbf{H}$ until torque balance expressed by $\mu_v H \sin\theta_v = \tau_v$ is achieved. If the former condition holds for $\theta=\pi/2$ (i.e., $\tau_v \geq \mu_v H$), the vortex line will continue to turn rigidly with the sample for all angles of rotation.

Hence, if there are many vortex lines and there is a distribution in the strength of the maximum pinning torque τ_v,[15] the possibility exists that some of the lines will continue to rotate rigidly with the sample while the rest will remain at various angles (θ_v) below $\pi/2$ relative to $\mathbf{H}$. In pursuing this possibility, we assume that the two groups of vortex lines can move freely relative to each other and do not become entangled.

We will therefore consider a superconducting sample that is turned by angle θ relative to $\mathbf{H}$ after field cooling and that contains N_v vortex lines of moment μ_v, of which $(1-\rho)N_v$ turn rigidly with the sample ($\theta_v=\theta$) and ρN_v lie at angles θ_v between zero and a maximum value θ_{vm}, where θ_{vm} equals θ if $\theta \leq \pi/2$ or equals $\pi/2$ if $\theta \geq \pi/2$. For simplicity, we assume that the maximum pinning torques on the vortex lines have a distribution in strength such that the ρN_v lines are oriented uniformly over the range $0 < \theta_v \leq \theta_{vm}$. In such a case, the incremental angle between any two adjacent lines

$$\theta' = \theta_{vm}/\rho N_v = \tfrac{1}{2}\pi/\alpha N_v \ ,$$

where the dimensionless parameter α, so defined, depends only on (and changes monotonically with) H, which becomes clear in what follows. The longitudinal magnetization component (parallel to $\mathbf{H}$) of these ρN_v lines involves a simple summation, which converts to an integration for ρN_v very large, such that

$$M_2^{(L)}=(\mu_v/\theta')\int_0^{\theta_{vm}}\cos\theta_v\,d\theta_v=(\mu_v/\theta')\sin\theta_{vm}\ .$$

Using $\mu_v/\theta'=2\alpha N_v\mu_v/\pi$, we obtain, for $M_2^{(L)}$ normalized by $N_v\mu_v$,

$$m_2^{(L)}=(2\alpha/\pi)\sin\theta_{vm}\ . \tag{1}$$

For the corresponding transverse magnetization component (normal to $\mathbf{H}$ in the plane of rotation), a similar procedure yields after normalization by $N_v\mu_v$,

$$m_2^{(T)}=(2\alpha/\pi)(1-\cos\theta_{vm})\ . \tag{2}$$

Regarding the $(1-\rho)N_v$ vortex lines that are turning rigidly with the sample, each of them contributes $\mu_v\cos\theta$ and $\mu_v\sin\theta$ to the longitudinal and transverse magnetization components, respectively. Hence, for the components normalized again by $N_v\mu_v$, we have

$$m_1^{(L)}=(1-2\alpha\theta_{vm}/\pi)\cos\theta \tag{3}$$

and

$$m_1^{(T)}=(1-2\alpha\theta_{vm}/\pi)\sin\theta\ , \tag{4}$$

where we have replaced ρ by $2\alpha\theta_{vm}/\pi$.

From Eqs. (1)–(4), it follows that, as θ is raised from 0 to $\pi/2$ (and θ_{vm} rises accordingly) the magnitude of the $\mathbf{m}_2$ vector grows from 0 to $2\sqrt{2}\alpha/\pi$ while the $\mathbf{m}_1$ vector diminishes in size from unity to $1-\alpha$. As θ is increased further from $\pi/2$ to 2π (and θ_{vm} stays at $\pi/2$), $\mathbf{m}_2$ remains as a vector of magnitude $2\sqrt{2}\alpha/\pi$ oriented at angle $\pi/4$ relative to $\mathbf{H}$, whereas $\mathbf{m}_1$ rotates rigidly with the sample with magnitude $1-\alpha$. This progression is represented schematically in the upper (increasing-θ) part of Fig. 7, which brings out the fact that, at $\theta=5\pi/4$ $(=225°)$, $\mathbf{m}_1$ and $\mathbf{m}_2$ are antiparallel and, hence, the total (normalized) vortex-flux magnetization $\mathbf{m}_P=\mathbf{m}_1+\mathbf{m}_2$ attains minimum size. This situation is extreme when $\mathbf{m}_1$ and $\mathbf{m}_2$ are of equal magnitude, so that $\mathbf{m}_P$ goes to zero, which occurs when $2\sqrt{2}\alpha/\pi=1-\alpha$, i.e., when α has the critical value

$$\alpha_c=(1+2\sqrt{2}/\pi)^{-1}\approx 0.526\ . \tag{5}$$

If we now consider what happens as θ is subsequently reduced from 2π to 0, it follows from our initial assumptions about the vortex-pinning torques that the orientational spread of vortex lines will turn such that $\mathbf{m}_2$ will rotate rigidly with the sample with magnitude $2\sqrt{2}\alpha/\pi$ until its angle relative to $\mathbf{H}$ reaches $7\pi/4$ $(=315°)$ at $\theta=3\pi/2$, where it will stay as θ continues to decrease to

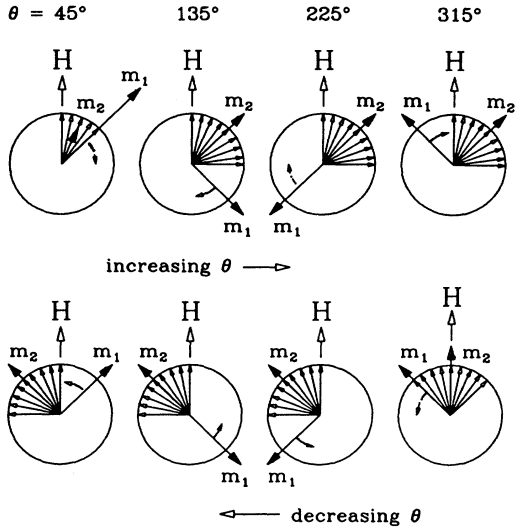

FIG. 7. Schematic depiction of $\mathbf{m}_1$ and $\mathbf{m}_2$ for increasing and decreasing sample-rotation angle θ. Vortex lines whose moments comprice $\mathbf{m}_1$ rotate rigidly with sample; those whose moments comprise $\mathbf{m}_2$ have orientational spread near field $\mathbf{H}$ and rotate frictionally relative to sample.

0. Hence, instead of Eqs. (1) and (2), we now have for $3\pi/2\le\theta\le 2\pi$,

$$m_2^{(L)}=(2\sqrt{2}\alpha/\pi)\cos(\theta+\pi/4) \tag{6}$$

and

$$m_2^{(5)}=(2\sqrt{2}\alpha/\pi)\sin(\theta+\pi/4)\ ,$$

and for $0\le\theta\le 3\pi/2$,

$$m_2^{(L)}=-m_2^{(T)}=2\alpha/\pi\ . \tag{7}$$

Furthermore, since $\mathbf{m}_1$ will continue to turn rigidly with the sample with magnitude $1-\alpha$, we have, for all values of θ,

$$m_1^{(L)}=(1-\alpha)\cos\theta,\ m_1^{(T)}=(1-\alpha)\sin\theta\ . \tag{8}$$

The progression for reverse sample rotation is schematized in the lower (decreasing-θ) part of Fig. 7. Here, the situation in which $\mathbf{m}_1$ and $\mathbf{m}_2$ are antiparallel (and $\mathbf{m}_P$ is of minimum size) clearly occurs at $\theta=3\pi/4$ $(=135°)$, where $\mathbf{m}_P$ will again be zero when $\alpha=\alpha_c$, as given in Eq. (5). The evident differences between the magnetization changes for increasing and decreasing θ correspond to a rotational hysteresis that stems directly from the frictional rotations relative to the sample of the vortex lines whose moments comprise $\mathbf{m}_2$.

To find the evolution in this hysteretic behavior explicitly, we calculated the longitudinal and transverse components of the total (normalized) vortex-flux magnetization $\mathbf{m}_P$ $(=\mathbf{m}_1+\mathbf{m}_2)$ from Eqs. (1)–(4) and (6)–(8) for increasing and decreasing θ, respectively, for different numerical values of α ranging through α_c. The components

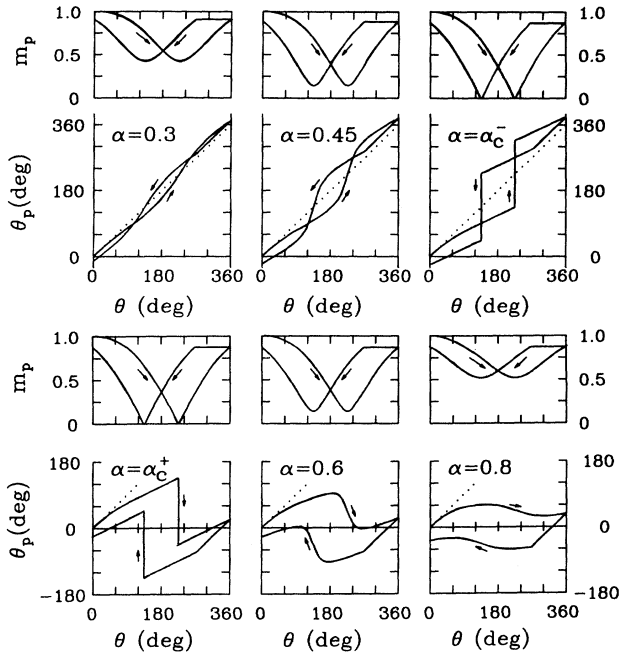

FIG. 8. Calculated m_P and θ_P vs θ for different values of α, as described in the text.

were then combined in quadrature to obtain the magnitude of $\mathbf{m}_P$ and its orientational angle θ_P relative to $\mathbf{H}$. The variations of m_P and θ_P over a complete rotational cycle in θ are displayed in Fig. 8 for various α, including α_c^- and α_c^+ (i.e., just below and just above α_c). As expected, for each α, m_P passes through a minimum value at $\theta=225°$ and 135° for increasing and decreasing θ, respectively, and the minimum m_P reaches down to zero at $\alpha=\alpha_c$. Equally striking, however, are the corresponding hysteretic changes in θ_P that occur near the θ values for minimum m_P. Specifically, the changes in θ_P get larger and more rapid at α increases to α_c^-, where they become discontinuous changes of 180°. Then, as α increases incrementally from α_c^- to α_c^+, the abrupt 180° changes of θ_P reverse in sign, and as α increases further, the reversed changes in θ_P become more gradual.

Since the parameter α is expected to vary directly with the external field H, it is evident that the calculated changes in m_P and θ_P versus θ with increasing α in Fig. 8 capture all the primary features of the experimental results for M_P and θ_P versus θ with increasing H shown in Figs. 2–4. Moreover, for a comparison with our experimental results for $M_P(\min)/M_P(2\pi)$ and $(d\theta_P/d\theta)^{-1}_{\max}$ shown in Fig. 6, we obtain from our analysis that

$$m_P(\min)=|1-\alpha/\alpha_c| \tag{9}$$

and

$$(d\theta_P/d\theta)^{-1}_{\max}=(1-\alpha/\alpha_c)/(1-\alpha)\ , \tag{10}$$

with α_c as given in Eq. (5). These two quantities (which occur at the same values of θ) both go to 0 at $\alpha=\alpha_c$, where $(d\theta_P/d\theta)^{-1}_{\max}$ changes sign, thus reproducing the basic experimental behavior displayed in Fig. 6. However, the curves in the latter figure are consistently displaced along H for the two directions of sample rotation, for which our model interpretation is that, at any given H the effective value of α is slightly larger for the reverse rotation than for the initial forward rotation. This would imply that, during the rotational cycle, there is a small decrease in the proportion of vortex lines that rotate rigidly with the sample.

Several other discrepancies between experiment and our simple model should be noted. First, a much larger initial drop in M_P with increasing θ is observed (Figs. 2–4) than is calculated for m_P (Fig. 8). Since the model assumes that the total number of vortex lines is conserved during the sample rotation, it would appear that the initial measured drop in M_P corresponds to an initial expulsion of vortex lines from the field-cooled sample, which is what we concluded from our earlier rotational experiments.[12] Secondly, the measured minima in M_P occur near $\theta=180°\pm25°$, whereas the calculated minima in m_P are at $\theta=180°\pm45°$. The latter θ values, however, are derived specifically from the simplifying assumption made about the distribution of vortex-pinning forces; a distribution with a greater preponderance of weaker pinning forces would shift the m_P minima closer to (yet still symmetrically about) $\theta=180°$. Thus, neither of these discrepancies undermines the essential validity of the model.

Hence, in summary, the central premise of our model (namely, that a pinning-force distribution produces a directional bifurcation of vortex lines under sample rotation in a magnetic field) appears to give a basically accurate and consistent interpretation of the observed rotational magnetization behavior of field-cooled polycrystalline $YBa_2Cu_3O_7$. Initially, we were concerned that the strong magnetic anisotropy of $YBa_2Cu_3O_7$ might be playing some unanticipated role in this extraordinary behavior. However, this appears not to be the case since our current rotational measurements on a field-cooled polycrystalline sample of cubic $(Ba,K)BiO_3$, whose anisotropy is weak, are revealing magnetization properties that are qualitatively very similar to those reported in this paper.

ACKNOWLEDGMENTS

We are grateful to D. G. Hinks and B. Dabrowski for providing us with the $YBa_2Cu_3O_7$ material of this study. The work at the University of Illinois at Chicago (UIC) was supported in part by the National Science Foundation under Grant No. DMR-87-22880.

[1]K. A. Müller, M. Takashige, and J. G. Bednorz, Phys. Rev. Lett. **58**, 1143 (1987); A. C. Mota, A. Pollini, P. Visani, K. A. Müller, and J. G. Bednorz, Phys. Rev. B **36**, 4011 (1987).

[2]J. F. Carolan, W. N. Hardy, R. Krahn, J. H. Brewer, R. C. Thompson, and A. C. D. Shaklader, Solid State Commun. **64**, 717 (1987).

[3]M. Tuominen, A. M. Goldman, and M. L. Mecartney, Phys. Rev. B **37**, 548 (1988).

[4]Y. Yeshurun and A. P. Malozemoff, Phys. Rev. Lett. **60**, 2202 (1988).

[5]Youwen Xu, M. Suenaga, A. R. Moodenbaugh, and D. O. Welch, Phys. Rev. B **40**, 10 882 (1989).

[6]I. A. Campbell, L. Fruchter, and R. Cabanel, Phys. Rev. Lett. **64**, 1561 (1990).

[7]Y. Wolfus, Y. Yeshurun, and I. Felner, Phys. Rev. B **37**, 3667 (1988); I. Felner, U. Yaron, Y. Yeshurun, G. V. Chandrashekhar, and F. Holtzberg, *ibid.* **40**, 5239 (1989).

[8]C. Giovannella, G. Collin, and I. A. Campbell, J. Phys. (Paris) **48**, 1835 (1987); L. Fruchter and I. A. Campbell, Phys. Rev. B **40**, 5158 (1989).

[9]D. E. Farrell, C. M. Williams, S. A. Wolf, N. P. Bansal, and V. G. Kogan, Phys. Rev. Lett. **61**, 2805 (1988).

[10]Rotational measurements were made of the torque and of the kinetic magnetic-flux changes along a fixed **H**; see C. Heiden, M. Fuhrmans, and R. Schäfer, J. Low Temp. Phys. **30**, 337 (1978), and references therein. Rotational measurements were also made of the kinetic magnetic-flux changes parallel and perpendicular to **H**; see R. Boyer, G. Fillion, and M. A. R. LeBlanc, J. Appl. Phys. **51**, 1692 (1980), and references therein.

[11]Liwen Liu, J. S. Kouvel, and T.O. Brun, Phys. Rev. B **38**, 11 799 (1988); J. Phys. (Paris) Colloq. **49**, C8-2189 (1988).

[12]Liwen Liu, J. S. Kouvel, and T. O. Brun, J. Appl. Phys. **67**, 4527 (1990).

[13]The vortex-flux and diamagnetic shielding components of the magnetization of polycrystalline $YBa_2Cu_3O_7$ have been shown experimentally to have very different spatial distributions in the sample, as might be expected. See J. P. Renard, C. Giovannella, L. Fruchter, and C. Chappert, Physica C **153 - 155**, 330 (1988); M. A. -K. Mohamed, J. Jung, and J. P. Franck, Phys. Rev. B **39**, 9614 (1989).

[14]Note that χ_0 is considerably smaller than (about one-half of) the perfect shielding value of $-1/4\pi$ (in units of emu/cm^3), as generally found for polycrystalline $YBa_2Cu_3O_7$ and reported in Ref. 12.

[15]Any inherent differences in the effective pinning torque between the vortex lines near the surface and those in the interior of the sample will contribute to the apparent width of the distribution, thus affecting our phenomenological model only quantitatively.